THEORY AND SIMULATION OF PHASE SPACE TRANSPORT IN BURNING PLASMAS

F. ZONCA, G. WEI

Center for Nonlinear Plasma Science and ENEA C. R. Frascati, Frascati, Italy

Institute for Fusion Theory and Simulation, School of Physics,

Zhejiang University, Hangzhou, China

Email: fulvio.zonca@enea.it

M. V. FALESSI

Center for Nonlinear Plasma Science and ENEA C. R. Frascati, Frascati, Italy Istituto Nazionale di Fisica Nucleare (INFN), Sezione di Roma, Piazzale Aldo Moro 2, Roma, Italy

L. CHEN

Institute for Fusion Theory and Simulation, School of Physics, Zhejiang University, Hangzhou, China
Department of Physics, National Central University, Taiwan
Center for Nonlinear Plasma Science and ENEA C. R. Frascati,
Frascati, Italy

P. LAUBER, A. BOTTINO, T. HAYWARD-SCHNEIDER, G. MENG

Max Planck Institute for Plasma Physics, 85748 Garching, Germany

S. BRIGUGLIO

Center for Nonlinear Plasma Science and ENEA C. R. Frascati, Frascati, Italy

A. MISHCHENKO

Max Planck Institute for Plasma Physics, 17491 Greifswald, Germany

Z. QIU

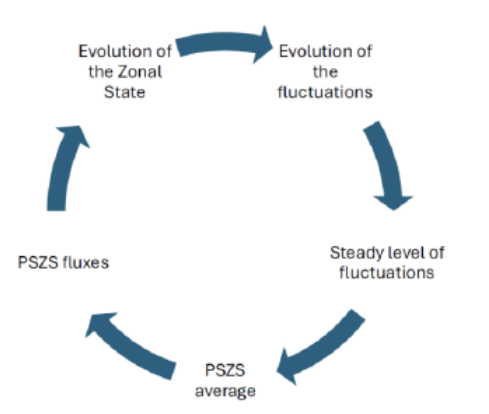
Institute of Plasma Physics, Chinese Academy of Sciences (ASIPP), Hefei 230031, China Center for Nonlinear Plasma Science and ENEA C. R. Frascati, Frascati, Italy

Abstract

This study reviews the role of phase-space zonal structures (PSZS) in burning plasmas, illustrating their evolution due to Alfvénic fluctuations using synthetic diagnostics with HMGC, GTC, and ORB5 codes. The results validate the ATEP code for simulating distribution function evolution in realistic tokamak conditions, including sources and collisions. The presented work demonstrates the existence of an overarching and unified theoretical framework for the self-consistent description of fluctuation spectra and corresponding transport in reactor-relevant fusion plasmas. The integration of the ATEP workflow into the ITER IMAS system is complete, and applications to realistic cases of practical interest are in progress.

1. INTRODUCTION

Reactor-relevant burning plasmas are complex, self-organized systems in which energetic particles (EPs) play a crucial role in processes underlying cross-scale couplings [1,2,3]. This study first reviews the concept of phase-space zonal structures (PSZS) [1,2,3] and their significance in transport analyses [4,5], particularly in burning plasmas. As a paradigm case, we illustrate the PSZS evolution due to energetic particle modes (EPMs) by means



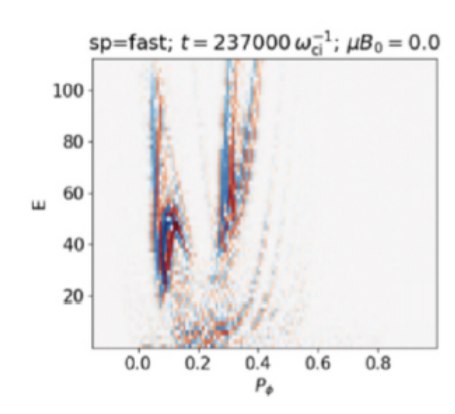


FIG. 1. Left Panel: Schematic diagram of a Phase-Space Zonal Structure (PSZS) transport workflow such as ATEP [8]. Right Panel: Example of EP PSZS ($\overline{F_0}^{(O)}$) defined as in Eq. (1)) as calculated by the ORB5 diagnostic [7] for $\mu=0$ in the (\mathcal{E}_0,P_ϕ) plane in units of $(c_S^2/2,-(e/c)\psi_w)$, with c_S the sound speed on the magnetic axis and ψ_w the magnetic flux at the wall (cf. SEC. 2).

of synthetic diagnostics originally developed for the hybrid code HMGC [6]. We also employ the PSZS diagnostics in the non-linear global gyrokinetic particle-in-cell code ORB5 [7] to verify results obtained by the phase-space transport code ATEP [8] and to illustrate phase-space transport features of the thermal plasma component. This study provides insights into the unique role of PSZS, which is crucial for accurately capturing transport dynamics with and without energetic particles.

When addressing fusion plasmas, slowly evolving local equilibria are typically assumed to be Maxwellian; therefore, transport studies involve solving 1D advection-diffusion equations where fluxes are calculated using various numerical workflows such as JINTRAC or TRANSP. However, when dealing with EPs and, more generally, with burning plasmas, it is necessary to generalize equilibrium and transport descriptions to accurately account for characteristic self-organization processes [1,2,3]. In Refs. [4,5], we established that the slowly evolving equilibrium distribution function is described by PSZS, whose governing equation can be derived using multiscale perturbation theory. As demonstrated in numerous analytical calculations (see, e.g., Ref. [4]), this approach allows us to describe the self-consistent modifications of the equilibrium on intermediate (meso-) spatiotemporal scales and the deviations from the local Maxwellian due to resonant transport. By taking the moments of the PSZS, we can recover the usual transport equations [5,9] in the proper limit. This analysis is crucially important because it enables us to consistently describe the EPs' equilibrium evolving over long time scales and the corresponding electromagnetic Zonal Fields level [4,5].

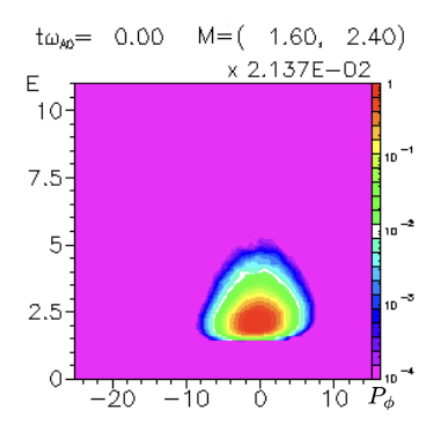
A phase-space transport workflow, analogous to the one described above, is therefore desirable. This is illustrated in the left panel of FIG. 1. Conceptually similar to the advection-diffusion equation solved in traditional transport workflows, the fluxes in this case must be described in the action phase space where the PSZS are defined, i.e., the single-particle constant of motion space. Restarting a global gyrokinetic code from PSZS and corresponding plasma equilibria, as calculated from the phase-space transport workflow, will allow for extending global gyrokinetic simulations over long time scales, similar to codes such as Trinity [9] or Gene Tango [10], but without postulating a model distribution function accounting for the proximity to local thermodynamic equilibrium.

We will demonstrate how a gyrokinetic code such as ORB5 [7] can be adopted to compute PSZS and their evolution for understanding the improvement of core confinement in the presence of a finite level of Alfvénic fluctuations. Additionally, we will illustrate ATEP [8] as a phase-space transport code capable of solving the workflow described in the left panel of FIG. 1, addressing in particular EP transport by Toroidal Alfvén Eigenmodes in the ITER 15MA case. The evolution of the PSZS will then be compared between two different layers of a hierarchy of transport models [11,12, 13]: nonlinear gyrokinetics solved by ORB5 and quasilinear fluxes solved by ATEP.

2. THE IMPORTANCE OF PHASE-SPACE TRANSPORT

Because the PSZS concept [1,2,3] generalizes the local Maxwellian equilibrium, PSZSs are 'slowly evolving' and unaffected by collisionless damping like Landau damping. They are computed via a two-step average: first, along guiding center orbits, and then filtering out fast fluctuations. PSZS thus depend solely on invariants such as energy $\mathcal{E}_0 = v^2/2$, the magnetic moment $\mu = v_\perp^2/2B_0$, and the toroidal angular momentum P_ϕ , with evolution expressed in terms of these invariants.

We introduce phase-space coordinates $\mathbf{Z} = (\theta, \zeta, P_{\phi}, \mathcal{E}_0, \mu)$, with θ and ζ being angle-like magnetic flux coordi-



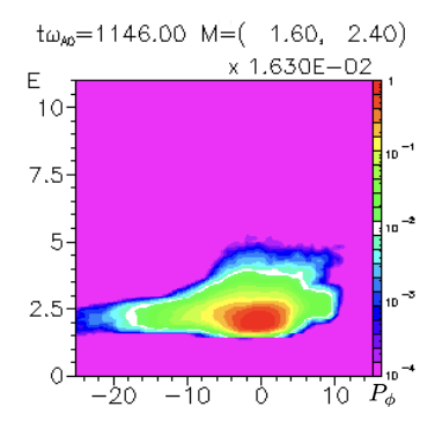


FIG. 2. Left Panel: EP PSZS in the linear unstable EPM phase. Right Panel: EP PSZS after the EPM burst and frequency chirping have occurred. Here, μ is fixed, time is given in units of the Alfvén frequency on the magnetic axis, while $(\mathcal{E}_0, \mu, P_\phi)$ are normalized to $(v_{EP}^2/2, v_{EP}^2/2\bar{B}_0, m_{EP}v_{EP}a)$, where v_{EP} is the EP thermal speed on the magnetic axis, \bar{B}_0 is the magnetic field intensity, m_{EP} is the EP mass, and a is the torus minor radius.

nates. The phase-space velocity \dot{Z} decomposes as $\dot{Z}_0 + \delta \dot{Z}$, where \dot{Z}_0 describes integrable motion in the reference magnetic field, and $\delta \dot{Z}$ accounts for plasma-induced fluctuations. The gyrokinetic equation in conservative form reads:

$$\frac{\partial}{\partial t}(DF) + \nabla_Z \cdot (D\dot{Z}_0 F) + \nabla_Z \cdot (D\delta \dot{Z} F) = 0,$$

where D is the velocity-space Jacobian. To describe the equilibrium evolution, the focus shifts to the toroidally symmetric ('zonal') distribution function F_z .

Using the magnetic field $\mathbf{B}_0 = \hat{F} \nabla \phi + \nabla \phi \times \nabla \psi$ with $\hat{F} = RB_{\phi}$, the equilibrium flow term simplifies to an expression involving flux coordinates. The divergence term for the equilibrium part becomes:

$$\nabla \cdot (D\dot{Z}_0 F)_z = \frac{1}{\mathcal{J}_{P_\phi}} \frac{\partial}{\partial \theta} \left(D\mathcal{J}_{P_\phi} F \, \dot{Z}_0 \cdot \nabla \theta \right)_z,$$

with $\mathcal{J}_{P_{\phi}}$ representing the Jacobian in magnetic flux coordinates, with P_{ϕ} naturally adopted instead of ψ . Averaging the zonal component over θ using $\mathcal{J}_{P_{\phi}}$ as weight and assuming slow equilibrium evolution yields:

$$\partial_t \oint d\theta \, \mathcal{J}_{P_{\phi}} DF_z + \oint d\theta \, \mathcal{J}_{P_{\phi}} \frac{\partial}{\partial Z} \cdot (D\delta \dot{Z}F)_z = 0,$$

where the orbit average

$$\overline{(\ldots)}^{(O)} = \frac{1}{\tau_b} \oint d\theta \, \frac{(\ldots)}{\dot{\theta}}$$

is performed over the bounce time τ_h .

In deriving the PSZS equation, the macro- and meso-scopic components lead to:

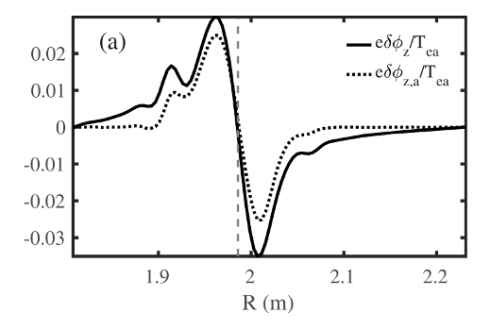
$$\frac{\partial}{\partial t}\overline{F_0}^{(O)} + \frac{1}{\tau_b} \left[\frac{\partial}{\partial P_\phi} \overline{\tau_b \delta \dot{P}_\phi \delta F}_z^{(O)} + \frac{\partial}{\partial \mathcal{E}} \overline{\tau_b \delta \dot{\mathcal{E}} \delta F}_z^{(O)} \right]_S = \overline{C}_S^{g(O)} + \overline{S}_S^{(O)}, \tag{1}$$

where $[...]_S$ indicates a suitable spatiotemporal averaging. Finally, the gyrocenter response decomposes as:

$$F_z = \overline{F_z}^{(O)} + \delta \tilde{F}_z = \overline{F_0}^{(O)} + \overline{\delta F_z}^{(O)} + \delta \tilde{F}_z, \tag{2}$$

with $\overline{F_0}^{(O)}$ representing a slowly evolving equilibrium, $\overline{\delta F_z}^{(O)}$ capturing microscale 'neighbouring equilibria' [14], and $\delta \tilde{F}_z$ being the residual term, which by construction has zero orbit average.

By definition, it is evident that Eq. (2) allows reconstructing PSZSs from any given toroidally symmetric gyrocenter distribution function [6,7]. In this sense, Eq. (2) can be considered a definition of PSZS once the proper spatiotemporal averaging has been introduced, also based on the physics problem of interest. However, Eq. (1) can be understood as a definition of PSZS as well, and, obviously, the two definitions are fully consistent, provided that proper accuracy is used in the orbit-averaging computation. This has been shown to be the case with explicit numerical computations by the HMGC code for the case of a nonlinearly evolving energetic particle mode (EPM)



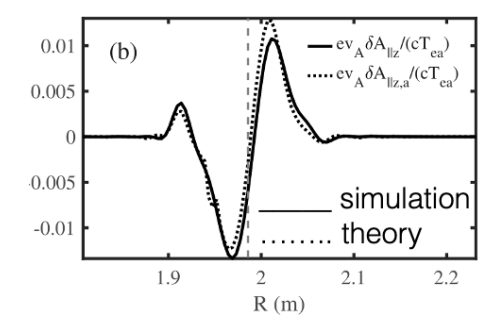


FIG. 3. Electromagnetic Zonal Fields (ZFs) obtained for a saturated RSAE [16]. The zonal scalar potential (left panel) and parallel vector potential (right panel) are both shown, comparing numerical simulation results with the theoretical/analytical predictions. The dashed vertical line denotes the vanishing magnetic shear radial location.

with frequency chirping [2,6]. For EPM, in particular, separating slow and fast spatiotemporal evolution loses its meaning since transport and nonlinear scales are the same and must be accounted for on the same footing [1,2,3] as illustrated in FIG. 2, showing PSZS given by $\overline{F_z}^{(O)} = \overline{F_0}^{(O)} + \overline{\delta F_z}^{(O)}$ in the initial (left panel) and final stage (right panel), after the EPM burst and frequency chirping have occurred.

The nonlinear equilibrium, or zonal state, consists of PSZSs and the corresponding electromagnetic Zonal Fields (ZFs), which are obtained from the proper quasineutrality condition and parallel Ampère's law [1,11], evolving on long time scales due to the combined effects of fluctuations, sources/sinks, and collisions [1,4,5]. The importance of phase-space transport and of phase-space features of the zonal state, characterizing its deviations from local thermodynamic equilibrium, is not only important for collisionless EPs but also for thermal plasmas. This was noted originally by Chen and Zonca in Ref. [14], discussing the properties of turbulent transport suppression by ZFs in the so-called 'Dimits shift' region, and more recently emphasized by Wang et al. in gyrokinetic numerical simulations of internal transport barrier formation in ion-temperature-gradient-driven turbulence [15]. To illuminate this case, we remind the reader of the recent results obtained in Ref. [16] about the saturation of EP-driven reversed-shear Alfvén eigenmode (RSAE), which is of great relevance. RSAEs can be considered a paradigm for Alfvénic fluctuations dominating the core of reactor-relevant plasmas [17,18]. Consistent with numerical simulation results, theoretical studies demonstrate that ZFs, which are dominated by the zonal current, enhance the EP drive via PSZSs. Figure 3 shows the scalar potential (left panel) and the parallel vector potential (right panel), comparing numerical simulation results obtained with the GTC code with the theoretical/analytical predictions [16]. It can also be shown that zonal flow has a negligible effect on EP resonance detuning (shearing) in this case. More recently, it has been shown that saturation takes place via a downward frequency shift and enhanced damping due to core plasma effects.

3. CROSS-SCALE COUPLINGS IN ION-TEMPERATURE-GRADIENT-DRIVEN PLASMA TURBULENCE

In the existing theoretical framework [1,2,3], it has been demonstrated that EPs play a fundamental role as mediators in cross-scale couplings between micro-scale turbulence and saturated meso-scale EP-driven Alfvénic fluctuations. This may be due to the dependence of the linear growth rate of micro-scale turbulence on β (the ratio of kinetic to magnetic energy density), but, in particular, this may be due to the indirect coupling of micro- and meso-scale fluctuations mediated by ZFs [19,20]. Nonlinear gyrokinetic simulations with the ORB5 code demonstrate a clear reduction in the heat flux for both the bulk ions and the electrons, as shown in FIG. 4. Meanwhile, in FIG. 5, the overall heat flux is shown to be reduced in the presence of an EP population. This is the typical condition observed in gyrokinetic numerical simulation at small or moderate plasma β , where mode structures evolve from typical linear unstable modes to fully developed turbulence, as shown in FIG. 6. When β is further increased, the properties of the zonal state become more global and the impact of EP presence on transport may change significantly. This is shown in FIG. 7, where ORB5 simulations show that the EP heat flux becomes substantial at $\beta_e = 0.24\%$, and the total heat flux is by no means reduced, unlike in FIG. 5. Figure 8, which comparatively shows mode structures in the nonlinear phase without (left panel) and with (right panel) EP contribution to the dynamics, clearly suggests that the different behaviours are to be attributed to the presence of more global, electromagnetic, and nearly flute-like fluctuation structures. Meanwhile, in FIG. 9, the presence of EPs clearly yields stronger excitation of finite parallel electric field fluctuations with predominant Alfvénic polarization; that is, of kinetic Alfvén waves (KAWs) that are radially propagating. These simulation results suggest that the properties of the zonal state become increasingly more global as plasma β is increased. In particular, mesoscale phenomena are mediated by the EP PSZSs, which impact the corresponding ZFs. Meanwhile, these global properties of the

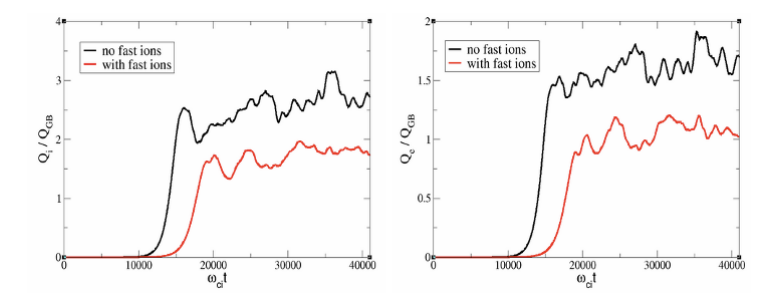


FIG. 4. Evidence of a reduction in the normalized perturbed energy flux in ion and electron channels due to the presence of EPs in ORB5 simulations. Energy fluxes are given in gyro-Bohm units, and the reference value is $\beta_e = 0.1\%$.

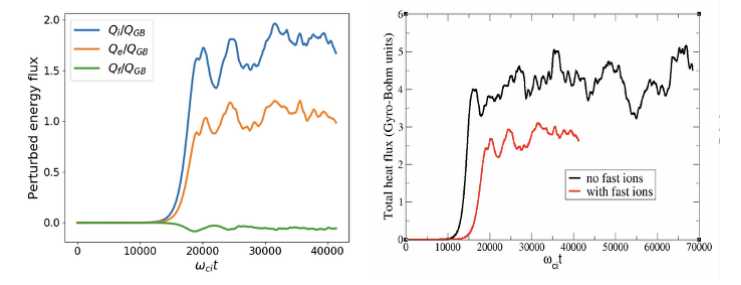


FIG. 5. Same simulation as in FIG. 4. Here, the normalized perturbed energy flux is also shown in the EP channel. The total energy flux (right) is reduced in the presence of EPs.

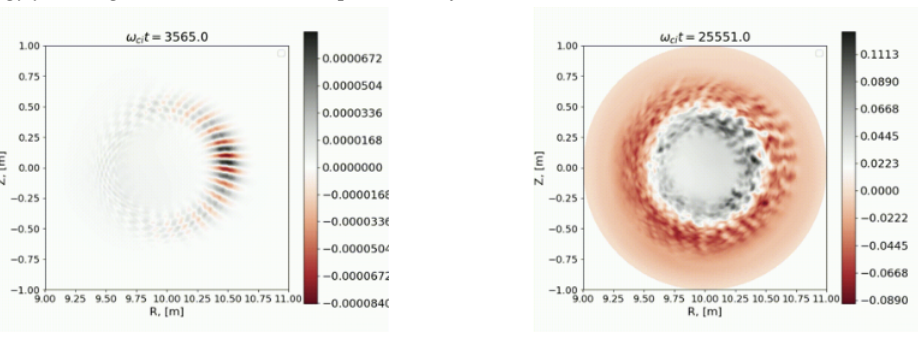


FIG. 6. Typical fluctuation structures for the simulations in FIGS. 4 and 5. The mode structure in the linear instability phase (left) evolves to fully developed turbulence at later times (right).

zonal states are intimately connected with radially extended flute-like fluctuation structures and KAW propagation, which must be properly captured for an accurate description of these physics. A need for electromagnetic global nonlinear gyrokinetic simulations for accurately describing these physics is stressed by this point.

4. A WORKFLOW FOR PHASE-SPACE TRANSPORT COMPUTATION: THE ATEP CODE

Equation (1) has been implemented in a numerical workflow to simulate the evolution of the distribution function based on realistic tokamak experimental conditions. The suite of codes and algorithms used to solve for advanced energetic particle transport models consistent with the general theoretical framework discussed above is known under the acronym ATEP [8].

The ATEP code and the corresponding EP workflow are fully integrated within the ITER Integrated Modelling & Analysis Suite (IMAS); that is, they are available as part of the collection of software used at ITER for all physics modelling and analysis. To illustrate the capability of ATEP and the EP workflow, FIG. 10 (left) shows the electrostatic potential of the n=13 toroidal Alfvén eigenmode (TAE) with f=75.5 kHz as calculated with LIGKA [8]. The corresponding PSZS is shown as a deviation from the initial distribution function, assuming a constant amplitude $\delta B/B_0=1\times 10^{-5}$, respectively, in the (P_ϕ,E) plane (middle, integrated over $\Lambda\equiv \mu B_0/E$) and in the (E,Λ) plane (right, integrated over P_ϕ).

In these simulations, the reference EP distribution function (hydrogen) in ITER's off-axis beam configuration (#100015/1) is assumed from original marker data as computed by the NEMO/SPOT package. The data was then

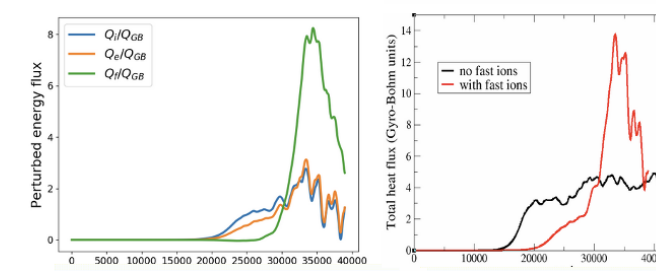
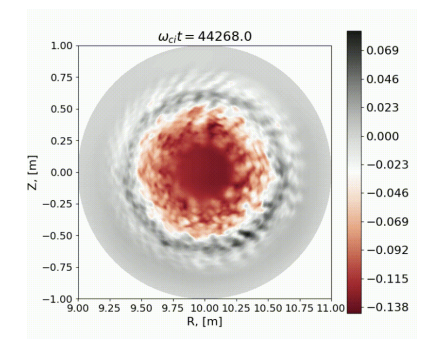


FIG. 7. Evidence of a substantial increase in the EP-normalized perturbed energy flux in ORB5 simulations. Energy fluxes are given in gyro-Bohm units, and the reference value is $\beta_e = 0.24\%$.



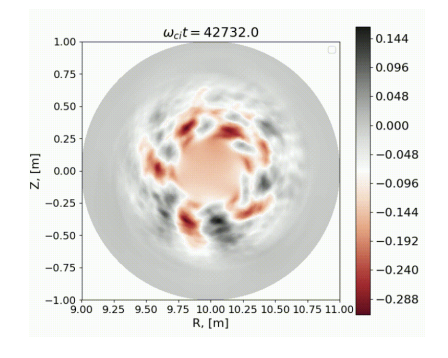


FIG. 8. Same simulation as in FIG. 7. Here, the presence of EPs clearly yields more global, electromagnetic, and nearly flute-like fluctuation structures.

binned, smoothed, splined, and projected onto the regular (P_{ϕ}, E, Λ) grid of the ATEP code, with corresponding smooth values of the distribution function and derivatives, as shown in FIG. 11 for the slice at $\Lambda = 0.5$ [8].

To demonstrate the capability to simulate realistic conditions, great efforts have been devoted to incorporating sources and collisions in Eq. (1) [21]. Figure 12 illustrates the time evolution of the EP distribution function as given by ATEP-3D when solving Eq. (1) without fluctuation-driven fluxes. A comparison with the asymptotic distribution function given by SPOT shows excellent agreement.

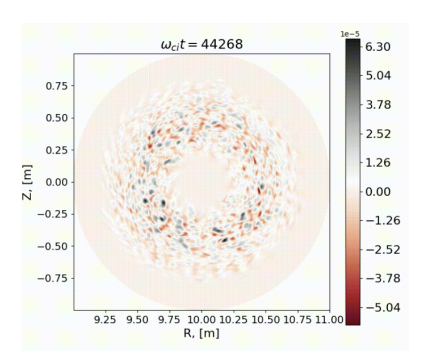
Phase-space fluxes computed with ATEP-3D and ORB5 demonstrate a good level of consistency for both single-mode and multi-mode cases. Phase-space zonal structures, shown as a deviation from the initial distribution function, are shown in FIG. 13 as a function of canonical toroidal momentum and energy for passing particles, calculated by LIGKA/ATEP (left) and ORB5 (right). An ITER NBI case with two TAEs with n=18 and n=19 is illustrated here in the non-linear saturation phase. The slight discrepancy between PSZSs computed by LIGKA/ATEP and ORB5 at low energy is to be attributed to the test-particle approach used for computing phase-space fluxes in ATEP-3D, which does not properly render higher-order resonances. This issue can be easily addressed. Furthermore, as a general algorithm to solve for phase-space transport as formulated in Eq. (1), ATEP-3D allows for different levels of approximation, both in the evaluation of fluctuation-driven phase-space fluxes and in the calculation of source and collision effects. Direct interfaces to standard one-dimensional transport codes via effective EP diffusion coefficients and moments of F_{EP} have been established, allowing for seamless integration in comprehensive transport frameworks [22].

5. CONCLUDING REMARKS AND DISCUSSION

This work demonstrates a comprehensive theoretical framework for the self-consistent modeling of fluctuation spectra and transport in reactor-relevant fusion plasmas. The framework is based on the phase-space zonal structure (PSZS) concept, which provides a unified approach to describing equilibrium distribution functions and their evolution under the influence of energetic particles and turbulence.

Numerical applications have been performed for selected reference cases, using codes like HMGC, ORB5, and ATEP. Verification efforts, including comparisons between ATEP-3D and ORB5, demonstrate a good level of consistency in simulating phase-space fluxes and zonal structures. These results validate the numerical tools and the underlying theoretical approach, with the inclusion of source and collision terms.

Applications to realistic scenarios and extension to 3D confinement systems are underway. The ATEP code has been integrated into the ITER IMAS system, enabling its use for predictive modeling in ITER. Future work will



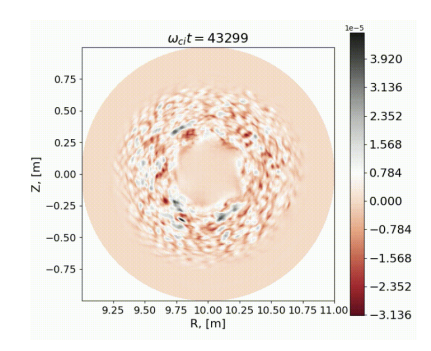


FIG. 9. Similar to FIG. 8, the presence of EPs (right) clearly yields stronger excitation of finite parallel electric field fluctuations with predominant Alfvénic polarization than without EPs (left); that is, of KAW that are radially propagating.

focus on enhancing the accuracy and applicability of the framework to practical fusion devices and on restarting a gyrokinetic code such as ORB5 from a PSZS initial distribution function for the actual self-consistent modeling of fluctuation spectra and transport in reactor-relevant fusion plasmas, including source and collision terms.

ACKNOWLEDGEMENTS

This work has been supported in part by the Italian Ministry of Foreign Affairs under Grant No. CN23GR02, the National Natural Science Foundation of China under Grant No. 12261131622 and by INFN - CSN4 (Commissione Scientifica Nazionale 4 - Fisica Teorica) MMNLP project. This work has also partly been carried out within the framework of the EUROfusion Consortium, funded by the European Union via the Euratom Research and Training Programme (Grant Agreement No. 101052200EUROfusion). Views and opinions expressed are, however, those of the author(s) only and do not necessarily reflect those of the European Union or the European Commission. Neither the European Union nor the European Commission can be held responsible for them.

REFERENCES

- [1] CHEN, L., and ZONCA F. 2016 Rev. Mod. Phys. 88 015008
- [2] ZONCA, F. et al. 2015 New J. Phys. 17 013052
- [3] ZONCA, F. et al. 2015 Plasma Phys. Contr. Fusion 57 014024
- [4] FALESSI, M. V., and ZONCA F. 2019 Phys. Plasmas 26 022305
- [5] FALESSI, M. V., CHEN, L., QIU, Z., and ZONCA F. 2023 New J. Phys. 25 123035
- [6] BRIGUGLIO, S. et al. 2014 Phys. Plasmas 21 112301
- [7] BOTTINO, A. et al. 2023 J. Phys.: Conf. Ser. 2397 012019
- [8] LAUBER, P. et al. 2024 Nucl. Fusion 64 096010
- [9] ABEL, I. G. et al. 2013 Rep Prog Phys. 76 116201
- [10] PARKER, J. B. et al. 2024 Nucl. Fusion 58 054004
- [11] ZONCA, F. et al. 2021 J. Phys.: Conf. Ser. 1785 012005
- [12] WEI, G. et al. 2024 Phys. Plasmas 31 072505
- [13] WEI, G., et al. 2025 Nucl. Fusion 65 in press https://doi.org/10.1088/1741-4326/ae0803
- [14] CHEN, L., and ZONCA F. 2007 Nucl. Fusion 47 S727
- [15] WANG, S., WANG, Z., and WU T. 2007 Phys. Rev. Lett. 132 065106
- [16] CHEN, L., et al. 2025 Nucl. Fusion 65 016018
- [17] WANG, T. et al. 2018 Phys. Plasmas 25 062509
- [18] WANG, T. et al. 2019 Phys. Plasmas 26 012504
- [19] CITRIN, J., and MANTICA P. 2023 Plasma Phys. Contr. Fusion 65 033001
- [20] QIU, Z. et al. 2025 Plasma Sci. Technol. 27 095101
- [21] MENG, G. et al. 2024 Nucl. Fusion 64 096009
- [22] LAUBER, P. et al. 2025 Oral presentation at the 29th EU-US Transport Workshop, Sept. 8-12 2025, Budapest, Hungary

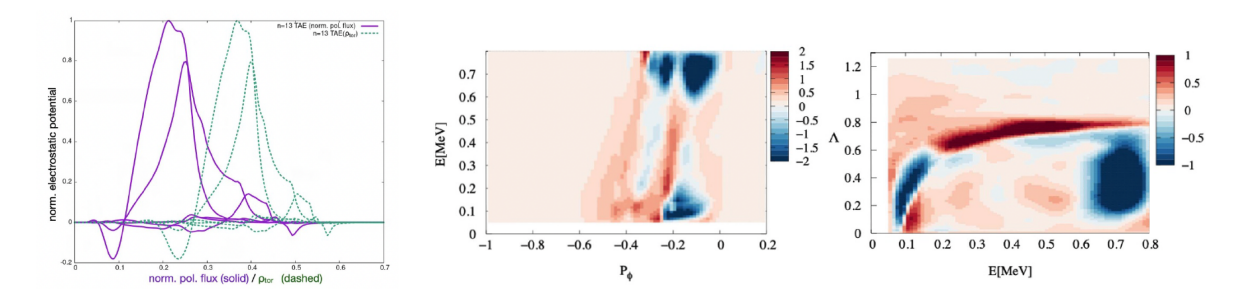


FIG. 10. Electrostatic potential of the n=13 TAE for the ITER 15 MA case (#100015/1, off-axis beam configuration). The corresponding PSZS is shown, respectively, in the (P_{ϕ}, E) plane (middle, integrated over $\Lambda \equiv \mu B_0/E$), and in the (E, Λ) plane (right, integrated over P_{ϕ}) [8].

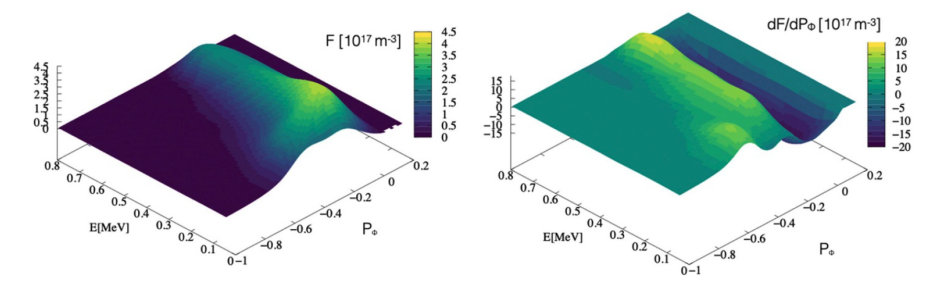


FIG. 11. Reference EP distribution function at $\Lambda=0.5$ in ITER's off-axis beam configuration (#100015/1) from original marker data as computed by the NEMO/SPOT package. The data was then binned, smoothed, splined, and projected onto the regular (P_{ϕ}, E, Λ) grid of the ATEP code, with corresponding smooth values of the distribution function and derivatives [8].

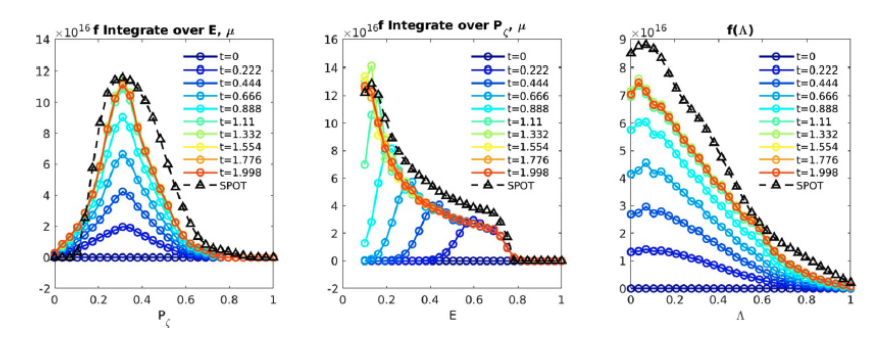


FIG. 12. Time evolution of the EP distribution function as given by the ATEP-3D code. Circle markers in different colors represent the time evolution, while the black dashed line with triangle markers represents SPOT simulation results for the time-asymptotic distribution function [21].

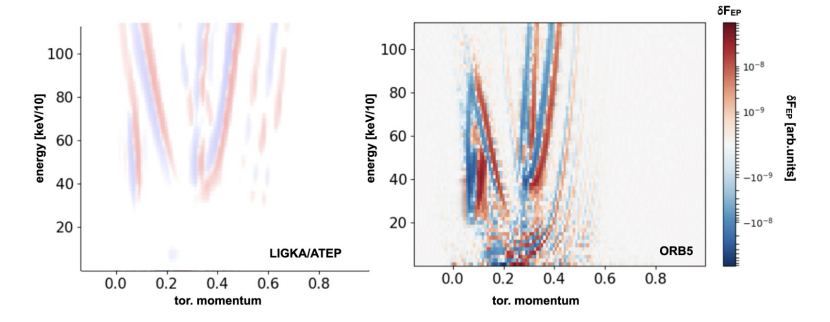


FIG. 13. Phase-space zonal structures as a function of canonical toroidal momentum and energy for passing particles, calculated by LIGKA/ATEP (left) and ORB5 (right), are compared. An ITER NBI case with two TAEs with n = 18 and n = 19 is illustrated here in the non-linear saturation phase [8].